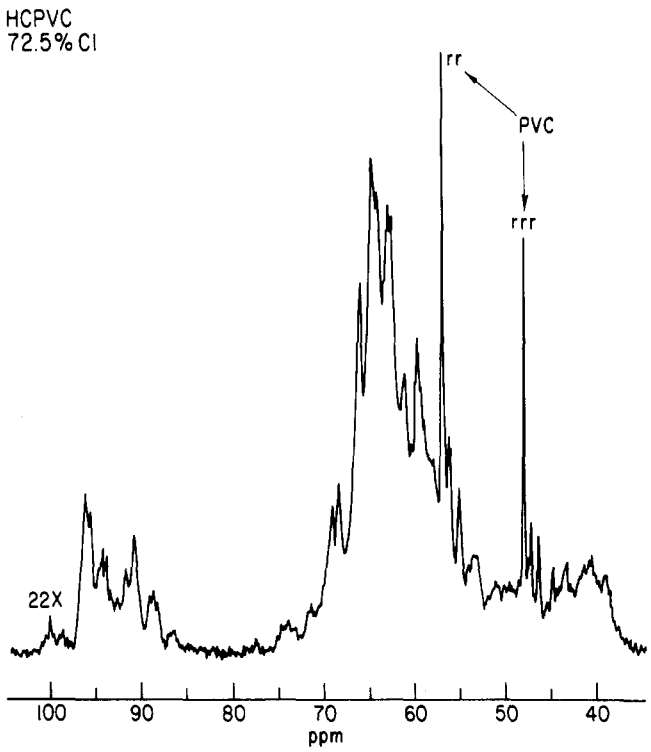

Figure 10. Very highly chlorinated CPVC prepared by a fluid bed process.

of a 73% chlorine CPVC produced by an experimental fluid-bed process.[25] Although our detailed analysis is not applicable at such a high chlorine level, two important observations can be noted from the spectrum. First, the syndiotactic PVC peaks are clearly visible and constitute at least 62–65% of the total area attributable to residual PVC (Table III). The results for this polymer confirm the reduced chlorination of the PVC crystallites relative to the amorphous regions in a heterogeneous process. In addition, a new CCl_2 peak appears at about 100 ppm which we assign to the presence of {22X} sequences. Obviously such sequences will be difficult to generate in measurable concentration under all but the most forceful chlorination conditions. No evidence for adjacent CCl_2 carbons was seen in a recent study of the chlorination of poly(vinylidene chloride).[26]

Acknowledgment. We thank Dr. M. H. Lehr (The BF Goodrich Co.) for helpful discussions concerning our results, Dr. W. E. Hull (Bruker Analytische Messtechnik) for obtaining the 100-MHz ^{13}C NMR spectra, and Dr. E. J. DeWitt (The BF Goodrich Co.) for providing the very highly chlorinated CPVC. We also thank a reviewer for helpful comments concerning eq 4–14.

References and Notes

(1) R. A. Komoroski, R. G. Parker, and M. H. Lehr, *Macromolecules*, **15**, 844 (1982).
(2) K. J. Ivin, *Pure Appl. Chem.*, **55**, 1529 (1983).
(3) R. A. Komoroski, S. E. Horne, Jr., and C. J. Carman, *J. Polym. Sci., Polym. Chem. Ed.*, **21**, 89 (1983).
(4) F. Keller and B. Hösselbarth, *Faserforsch. Textiltech.*, **29**, 152 (1978), and references therein.
(5) R. A. Komoroski and J. P. Shockcor, *Macromolecules*, **16**, 1539 (1983).
(6) J. B. Stothers, "Carbon-13 NMR Spectroscopy", Academic Press, New York, 1972.
(7) F. Keller, S. Zepnik, and B. Hösselbarth, *Faserforsch. Textiltech.*, **29**, 490 (1978).
(8) J. C. Randall, "Polymer Sequence Determination", Academic Press, New York, 1977, Chapter 3.
(9) F. Keller and B. Hösselbarth, *Faserforsch. Textiltech.*, **27**, 453 (1976).
(10) F. Keller, B. Hösselbarth, and C. Mügge, *Plaste Kautsch.*, **31**, 187 (1984).
(11) N. Colebourne and E. S. Stern, *J. Chem. Soc.*, 3599 (1965).
(12) R. G. Parker and G. A. Martello, "Encyclopedia of PVC" 2nd ed., L. I. Nass and C. H. Heiberger, Eds., in preparation.
(13) J. Gianelos and E. Grulke, *Adv. X-ray Anal.*, **22**, 473 (1979).
(14) C. J. Carman, *Macromolecules*, **6**, 725 (1973).
(15) F. A. Bovey, "High Resolution NMR of Macromolecules", Academic Press, New York, 1972, Chapter 3.
(16) F. Keller, *Faserforsch. Textiltech.*, **29**, 133 (1978).
(17) R. G. Parker, The BF Goodrich Co., U.S. Patent 4 350 798, Sept 21, 1982.
(18) R. G. Parker, The BF Goodrich Co., U.S. Patent 4 377 459, March 22, 1983.
(19) M. L. Dannis and F. L. Ramp, The BF Goodrich Co., U.S. Patent 2 996 489, Aug 15, 1961.
(20) A. J. Olson and R. G. Vielhaber, The BF Goodrich Co., U.S. Patent 4 412 898, Nov 1, 1983.
(21) W. Trautvetter, *Kuntstst-Plast. (Solothurn, Switz.)* **13**, 54 (1966).
(22) F. Keller, H. Opitz, B. Hösselbarth, D. Beckert, and W. Reicherdt, *Faserforsch. Textiltech.*, **26**, 329 (1975).
(23) J. Millan, *J. Macromol. Sci., Chem.*, **A12**, 315 (1978).
(24) A. Dorrestyn, P. J. Lemstra, and H. Berghmans, *Polym. Commun.*, **24**, 226 (1983).
(25) E. J. DeWitt, The BF Goodrich Co., unpublished results.
(26) R. T. Sikorski and E. Czerwińska, *Polymer*, **25**, 1371 (1984).

Thermal Property–Structure Relationships of Solution-Chlorinated Poly(vinyl chlorides)

Marvin H. Lehr,* Richard G. Parker, and Richard A. Komoroski

The BFGoodrich Research and Development Center, Brecksville, Ohio 44141.
Received September 7, 1984

ABSTRACT: The specific heat capacity increment (Δc_p) at T_g for the chlorinated poly(vinyl chlorides) (CPVC's) studied decreased almost continuously with increasing chlorine substitution. The decrease exceeded that calculated from the "constant molar bead heat capacity rule". This is interpreted as evidence that chlorine substitution stiffens the CPVC chain. At first chlorination up to 59% chlorine caused an increase in Δc_p, which coincided with the large initial decrease in PVC crystallinity. The crystallinity dropped to less than one-tenth the value in PVC when the chlorine level reached 61%. The relative drop in crystallinity coincided with the decrease in PVC syndiotactic sequences containing 12 or more monomer units as calculated from random chlorination statistics. Detectable crystallinity persisted until the chlorine content was about 67.5%. The Δc_p for 100% amorphous PVC was found to be in good agreement with theory.

Introduction

The early characterization and uses of solution-chlorinated poly(vinyl chloride) have been described by Bier[1] and Trautvetter.[2] They concluded that chlorine substitution was random or homogeneous compared to water-slurry or solvent-swollen chlorination processes, which gave

0024-9297/85/2218-1265$01.50/0

Table I
Thermal Properties of Virgin and Precipitated PVC's

sample	T_g, °C	ΔHm_2, kJ/kg	Δc_p, J/(g K)	ΔC_p(bead), J/(mol K)	wt loss at 150–200 °C, %
103EP-F76, lot 1 virgin	90.6	8.9 ± 1.3	0.347 ± 0.004	10.8 ± 0.2	
precipitated					
series 1	89.9	8.1 ± 0.3	0.368 ± 0.021	11.5 ± 0.7	0.1
series 2	91.5	8.2 ± 0.4	0.364 ± 0.004	11.4 ± 0.2	0
103EP-F76, lot 2 virgin	91.3	8.1 ± 0.1	0.347 ± 0.008	10.8 ± 0.3	
precipitated					
series 3	90.0	7.7 ± 0.5	0.347 ± 0.012	10.8 ± 0.4	

heterogeneous products of different properties. For example, when chlorinating two PVC's of different crystallinities in the water-slurry process, the one of higher crystallinity produced a CPVC of a higher Vicat softening point. However, when chlorinated in solution, the products had the same Vicat softening points, presumably because both crystalline and amorphous chains were equally accessible to chlorination.

In recent years many efforts have been made to elucidate the molecular structure of CPVC polymers by spectroscopic methods, in particular, through the use of ^{13}C NMR.[3,4] However, analysis has been difficult because of the structural complexity of the polymers and instrumental limitations. The recent availability of wide-bore, cryomagnet NMR systems has greatly improved spectral resolution and has helped in peak assignments using model polymers, specifically, lightly chlorinated PVC's, vinyl chloride/1,2-dichloroethylene copolymers, and vinyl chloride/vinylidene chloride copolymers.[5] The preceding paper[10] describes quantitative microstructural analyses for the polymers studied here.

In contrast to the many structural studies of CPVC by spectroscopic methods, the examination of CPVC by thermal methods has received less attention. The specific heat capacity of a 66.8% chlorine CPVC was measured by Wilski up to 150 °C.[6] He concluded the polymer contained no crystallinity. However, Bonnebat and DeVries[7] reported residual crystallinity in annealed commercial samples containing up to 68% chlorine. Hosselbarth et al.[8] correlated T_g with degree of chlorination for both suspension- and solution-chlorinated polymers; in addition they showed that the slope of the glass transition curve could be related to the chemical inhomogeneity in resins produced in a fluidized-bed chlorination.[9]

Experimental Section

CPVC's. The CPVC's were prepared as described previously[5] by using a Geon 103EP-F76 PVC (The BFGoodrich Co.). The various samples represent aliquot portions taken from three separate chlorinations. The samples were precipitated from tetrachloroethane with excess methanol and dried overnight in a vacuum oven at 70–80 °C. Before running differential scanning calorimetric (DSC) analyses, we checked the dried powders for residual solvent using thermal gravimetric analysis (TGA). Any solvent loss occurred in the 150–200 °C range. Except for two samples, 15 and 16, solvent loss usually amounted to less than 0.3%.

DSC. A Perkin-Elmer Model DSC-2B differential scanning calorimeter was used for calorimetric studies. Temperature calibrations were made by using indium (T_m = 429.8 K) and tin (T_m = 505.1 K) and were found to be within ±1.0 K. Occasionally, analytical-grade benzoic acid (T_m = 396.6 K) was used. The cell heat constant was checked in accordance with the manufacturer's manual by using the indium heat of melting (28.4 J/g). Heating and cooling rates were 40 K/min. Sample weight was usually about 15 mg. A sample was typically heated to 510 K in both first and second runs. Values reported for T_g represent midpoints of the transitions. For heat capacity measurements below and above T_g the instrument was calibrated according to the manual by using a sapphire standard. The measurements were made after conditioning the sample in the DSC by heating/cooling to/from 500 K at 20 K/min.

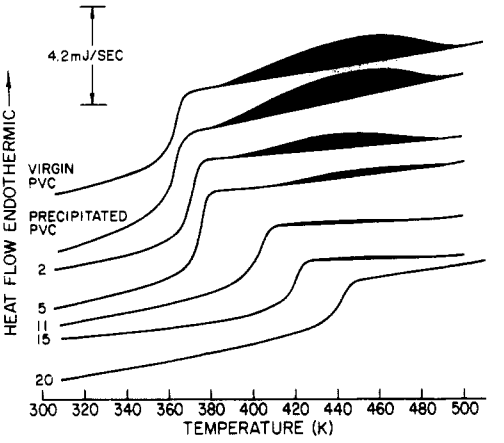

Figure 1. DSC second heat scans of PVC and solution-chlorinated PVC's.

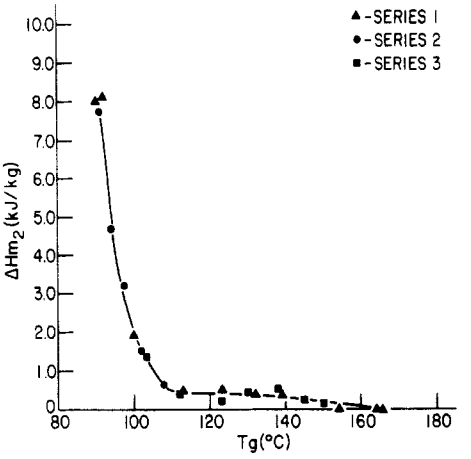

Figure 2. Second heat of melting vs. T_g of solution-chlorinated PVC's.

TGA. Thermogravimetric analyses were run under nitrogen gas at a heating rate of 30 K/min by using either a Cahn System 113 or a Perkin-Elmer TGS-2 instrument.

NMR. Carbon-13 NMR spectra were obtained at 50.3 MHz on a Bruker WH-200 wide-bore, cryomagnet FT NMR spectrometer as described previously.[5] The compositional analyses were determined by using the published procedure.[10]

Results and Discussion

Residual Crystallinity. The thermal property data were determined from the second heat run and are compiled in Table I for PVC and Table II for the CPVC's. The DSC second heat scans for some selected samples are shown in Figure 1. The shaded areas encompass the melting range of residual PVC crystallites. The extent of recrystallization as measured in the second heat of melting (ΔHm_2) is shown in Figure 2. A very rapid decrease in crystallinity occurred initially upon chlorination to about 61% chlorine (T_g = 110 °C). Crystallinity was reduced to

Table II
^{13}C NMR and Thermal Properties of Solution-Chlorinated PVC's

sample	% Cl wet	% Cl NMR	mol % CH_2	mol % CHCl	mol % CCl_2	M(bead)	T_g, °C	ΔHm_2, kJ/kg	Δc_p, J/(g K)	ΔC_p, J/(K mol)	wt loss at 150–200 °C, %
1	57.7	57.7	48.0	52.0	0.0	31.94	94.3	4.68 ± 0.06	0.376 ± 0.016	12.0 ± 0.5	0
2	58.7	58.7	46.4	53.1	0.5	32.66	97.5	3.26 ± 0.25	0.381 ± 0.008	12.4 ± 0.3	0.1
3	59.0	58.9	46.1	53.2	0.7	32.84	100.2	1.92 ± 0.13	0.376 ± 0.012	12.4 ± 0.4	0
4	59.5	59.5	44.7	54.8	0.5	33.25	101.6	1.55 ± 0.17	0.372 ± 0.016	12.4 ± 0.5	0.35
5	59.3	59.6	44.5	54.9	0.6	33.25	103.0	1.38 ± 0.21	0.376 ± 0.008	12.5 ± 0.3	0.3
6	60.5	60.6	43.9	53.8	2.3	34.15	107.8	0.63 ± 0.21	0.351 ± 0.020	12.0 ± 0.7	0
7	62.0	61.4	41.1	57.5	1.4	34.80	111.9	0.38 ± 0.04	0.347 ± 0.004	12.1 ± 0.1	0.1
8		62.0	40.6	57.2	2.3	35.34	113.2	0.42 ± 0.13	0.355 ± 0.004	12.6 ± 0.1	0
9	63.2	62.5	39.6	57.9	2.5	35.70	123.2	0.21 ± 0.21	0.305 ± 0.004	10.9 ± 0.2	0
10		63.5	37.5	59.5	3.0	36.60	123.4	0.54 ± 0.08	0.314 ± 0.016	11.5 ± 1.1	0
11	65.7	64.7	34.5	62.0	3.5	37.81	129.8	0.46 ± 0.03	0.297 ± 0.012	11.2 ± 0.5	0
12		65.0	33.7	62.7	3.6	38.12	132.3	0.42 ± 0.17	0.301 ± 0.016	11.5 ± 0.6	0
13	65.8	66.0	32.8	61.7	5.5	39.08	138.0	0.54 ± 0.04	0.276 ± 0.012	10.7 ± 0.5	0.25
14		66.4	30.7	64.6	4.7	39.53	139.4	0.38 ± 0.04	0.280 ± 0.004	11.0 ± 0.2	0.1
15	66.5	66.8	30.9	62.9	6.2	39.98	144.8	0.25 ± 0.04	0.247 ± 0.008	9.9 ± 0.3	0.75
16		68.4	25.9	67.4	6.6	41.79	149.3	0.17 ± 0.04	0.222 ± 0.004	9.3 ± 0.2	1.3
17	67.7	67.9	28.1	65.0	7.0	41.27	154.3	0	0.213 ± 0.008	8.8 ± 0.3	0.1
18	68.2	69.9	25.0	66.1	8.9	42.95	163.8	0	0.197 ± 0.004	8.4 ± 0.2	0
19	68.2	69.7	24.3	66.2	9.5	43.39	165.5	0	0.180 ± 0.004	7.8 ± 0.2	0.1
20	68.3	69.6	24.4	66.4	9.3	43.34	167.8	0	0.184 ± 0.004	8.0 ± 0.2	0.15

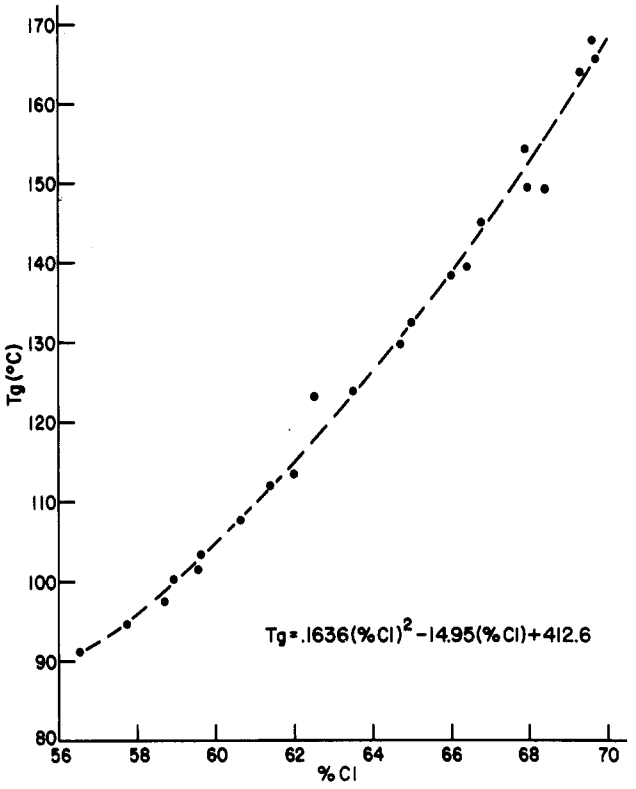

Figure 3. Glass transition temperatures vs. weight percent chlorine for CPVC's.

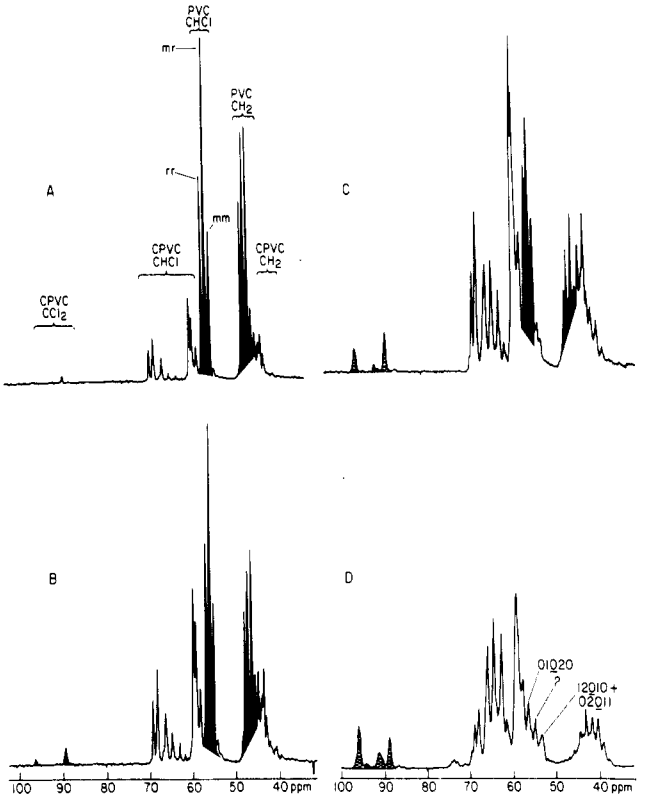

Figure 4. ^{13}C NMR spectra of selected CPVC's: A = sample 5, B = sample 9, C = sample 11, and D = sample 20 in Table II.

less than one-tenth its level in PVC. The results of Dorrestijn et al.[11] are in qualitative agreement with our observations. They found in dynamic mechanical measurements of CPVC/dioctyl phthalate gels that the solution-chlorinated PVC lost its ability to form a gel at about 60% chlorine. They speculated that at this point the average syndiotactic sequence length was reduced below a minimum value necessary for producing a network structure from crystallites. In our DSC measurements, detectable crystallinity persisted until the chlorine level reached about 67.5% chlorine (T_g = 150 °C).

^{13}C NMR Measurements. The results are compiled in Table II. The T_g vs. weight percent chlorine curve is shown in Figure 3. It is similar to data reported by Hosselbarth et al.[8] There is no T_g plateau about 63% chlorine as indicated by Trautvetter's data[2] for solution-chlorinated PVC's.

Selected spectra of samples at different stages in chlorine substitution are shown in Figure 4. Chlorine substitution produced initially only additional CHCl groups (58–70 ppm), which have been assigned to various five-carbon sequences.[5] Further substitution led to the appearance of a CCl_2-centered sequence at 89.5 ppm (crosshatched area, Figure 4A) in the form of an isolated vinylidene chloride structure (I). This sequence first appeared at about 57–58% chlorine. The large peaks (shaded areas) at 45–48 ppm (CH_2) and at 55–57 ppm (CHCl) arise from unchlorinated PVC sequences. The CHCl groups in syndiotactic (rr), heterotactic (mr), and isotactic (mm) sequences are so labeled in Figure 4A.

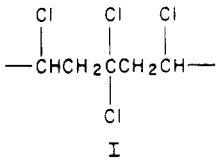

I

Above 61% chlorine, another CCl_2-centered sequence appeared near 96 ppm (Figure 4B). This was assigned to a CCl_2 in the center of a {01210} sequence,[5] structure II.

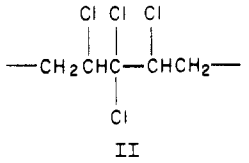

II

Further chlorine substitution led to enhancement of some peaks and diminution of others. At about 65% chlorine, the PVC peaks (shaded areas) in Figure 4C were much reduced. This is consistent with the low heat of melting (0.46 kJ/kg) of this sample.

Figure 4D shows the spectrum of sample 20 containing 68.3% chlorine. This sample showed little residual PVC. According to a more detailed analysis [sample 25, ref 10], it was estimated that this CPVC contained only about 4% PVC triads, which corresponds to only about 1% syndiotactic triads. The peak at 53.5 ppm might be confused with the center CHCl group of an isotactic triad {10101} at 55.5 ppm (Figure 4D); however, it has been assigned to the CH_2 group in the center of {12010} and {02011} sequences.[5,10] The peak at 55 ppm has not been positively assigned; the one at 56.5 ppm is due to a {01020} sequence and is the major interference to the experimental measurement of syndiotactic sequences using the CHCl-carbon region. The virtual absence of CH_2 peaks at 45–48 ppm indicates no vinyl chloride runs equal to or greater than four monomer units. The lack of any detectable melting in the fused sample is consistent with the NMR evidence of only 1% syndiotactic triads.

Calculation of Unchlorinated Vinyl Chloride Runs in CPVC. It has been shown that the tacticities of commercial PVC (polymerized at 50 °C) follow Bernouillian statistics.[12-14] This means that the addition of vinyl chloride monomer to a growing free-radical chain can be described by a single parameter (β), the probability of forming a syndiotactic diad, that is, a sequence of two monomer units having the syndiotactic configuration. The probability (α) of forming an isotactic diad is $1 - \beta$. Fox and Schnecko[15] determined that the mole fraction of syndiotactic diads in sequences of one or more is given by eq 1, where N is the number of diads. It is convenient to

$$f_{\geq N} = \beta^{N+1}(1 + \alpha N) \quad (1)$$

remember that $N = n - 1$, where n is the number of monomer units.

Since the syndiotactic ratio (S), namely the ratio of the syndiotactic triad peak at 57.5 ppm to the sum of all the tactic peaks at 56.5–57.5 ppm, remained relatively constant (0.29–0.33) up to and including sample 9 (Table IV), we assume chlorination was random with respect to PVC segments up to about 63% chlorine. We treat, therefore, chlorine-substituted diads as equivalent to isotactic diads, that is, noncrystallizable diads. The fraction of unchlorinated syndiotactic diads (β') can be expressed by eq 2, where m is the mole fraction of unchlorinated vinyl

$$\beta' = \beta m \quad (2)$$

chloride units. For example, if 80 mol % of the PVC monomer units are unchlorinated, we calculate for our PVC with $\beta = 0.537$ that $\beta' = (0.8)(0.537) = 0.430$, and $\alpha' = 1 - \beta' = 0.570$.

Table III
Calculated PVC Syndiotactic Sequences in CPVC for PVC Syndiotacticity = 0.537

m, mole fraction	n monomers mole fraction				
	≥4	≥6	≥8	≥10	≥12
1.0	0.199	0.078	0.029	0.010	0.0035
0.0	0.139	0.046	0.014	0.0039	0.0011
0.8	0.093	0.024	0.0058	0.0013	0.0003
0.7	0.057	0.012	0.0021	0.0004	
0.6	0.033	0.0049			

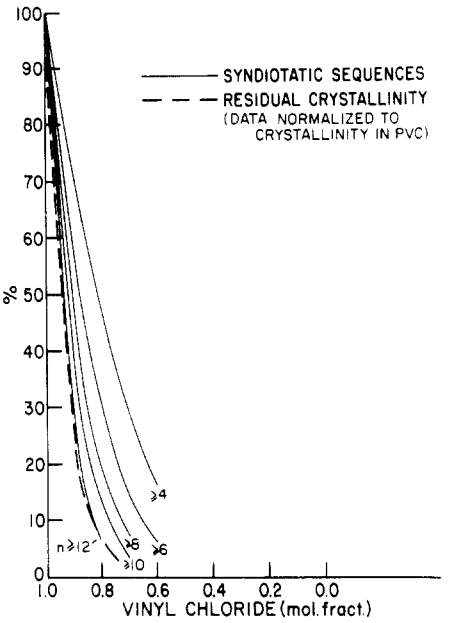

Figure 5. Residual crystallinity and PVC syndiotactic sequence lengths in CPVC (data normalized to unchlorinated PVC).

The literature contains various estimates of the number of PVC syndiotactic diads needed to crystallize, including a value as low as 4.[16] For our commercial PVC the fraction of syndiotactic sequences containing four or more diads is calculated from eq 1 as follows:

$$f_{\geq 4} = 0.537^5[1 + 0.463(4)] \quad (3)$$

$$f_{\geq 4} = 0.13 \quad (4)$$

And for a CPVC containing 80 mol % unchlorinated PVC, one obtains from eq 1 and 2 $\beta' = 0.048$. The calculations were carried out for various CPVC compositions between 100 and 60 mol % PVC monomer units, and for selected syndiotactic monomer sequence lengths from 4 to 12 units (Table III). The results are normalized to the values of PVC and plotted in Figure 5.

It is clear that long sequences are reduced more rapidly than short ones. This is expected because, for example, chlorine substitution in the middle of a sequence of 12 units gives two shorter sequences containing 5 and 6 units. Hence, as chlorine substitution proceeds, shorter syndiotactic sequences are partly replenished, but the longer ones are not.

It is instructive to compare the normalized sequence curves in Figure 5 with crystallinity data. For this purpose, the ΔHm_2 results (Table II) are also normalized to PVC, using $\Delta Hm_2 = 8.00$ kJ/kg, the average for the three precipitated PVC samples. To calculate the unchlorinated vinyl chloride fraction (m), we used the ^{13}C NMR data in Table II. We count each CH_2 group as part of an unchlorinated vinyl chloride unit. Since the CCl_2 group has

Table IV
PVC Syndiotactic Units in CPVC's

sample	T[a,b]	S[b]	m[c]	rr mole fraction found[d]	rr mole fraction calcd[e]
PVC	1.00	0.288	1.00	0.288	
1	0.871	0.286	0.960	0.249	0.261
2	0.792	0.292	0.918	0.231	0.234
3	0.739	0.299	0.908	0.221	0.227
4	0.729	0.301	0.884	0.219	0.213
5	0.682	0.317	0.878	0.216	0.208
6	0.554	0.296	0.832	0.164	0.181
7	0.511	0.330	0.794	0.168	0.161
8	0.473	0.328	0.766	0.155	0.146
9	0.378	0.323	0.742	0.122	0.134
10	0.342	0.305	0.690	0.104	0.111
11	0.260	0.366	0.620	0.095	0.083
12	0.253	0.366	0.602	0.093	0.077
13	0.195	0.400	0.542	0.078	0.058

[a] T = fraction of PVC triads remaining. [b] Determined from NMR data.[10] [c] Equation 5. [d] T × S. [e] Determined from eq 1 and 2.

been shown to appear first as an isolated vinylidene chloride unit, we correct for it as follows (eq 5), where m_0

$$m = (m_0 - m_2)/50 \quad (5)$$

is mole percent CH_2 groups and m_2 is mole percent CCl_2 groups. This assumption becomes less valid at higher chlorine levels where {021} and {121} structures become significant (sample 11, Figure 4C). For samples 1–9, where the CCl_2 content is no more than 2.5 mol %, the calculated and experimentally found values (Table IV) for PVC syndiotactic units triads (rr) agree within an average of 5%, confirming the assumption in eq 2 and the applicability of eq 1 to the random chlorination of PVC, at least up to 63% chlorine.

The results in Figure 5 show that under our conditions the normalized decrease in crystallized syndiotactic sequences superimposes the normalized syndiotactic sequence curve for $n \geq 12$. When only 20 mol % of the units were chlorinated (about 61% chlorine), both the heat of melting and syndiotactic sequences $n \geq 12$ were reduced to less than 10% of the level in the starting PVC. In terms of mole fractions, the sequences $n \geq 12$ are reduced from 0.35% in PVC to 0.03% in the CPVC (Table III). Since we determined that our PVC sample contained 15% crystallinity in the second heat run (see below), the above results indicate that the extent of crystallization of shorter sequences depends on the concentration of longer sequences. This could occur if the latter were acting as the seeds for nucleation. It is interesting to note that Keller and co-workers,[14,17] who investigated crystallinity in stretched PVC gels, concluded that a minimum of 14 repeat units were involved in the network forming crystals. In related work, Guerrero and Keller[18] recognized the large difference between percent crystallinity and the concentration of long syndiotactic sequences in commerical PVC. To reconcile the difference they suggested that the sequence distribution in PVC does not follow Bernoullian statistics beyond a certain length and that there exist in PVC a preponderance of longer syndiotactic runs, so in effect PVC is a block copolymer of amorphous and crystalline segments. Our results in Figure 5, showing a direct correlation between the decrease in crystallinity and calculated concentration of long syndiotactic sequences, indicate that Bernoullian statistics are obeyed.

The effect of crystallinity on the solubility of PVC has been shown to be significant. Commercial PVC is insoluble in acetone.[19,20] However, solution-chlorinated PBC containing 62–64% chlorine (20–30% chlorinated monomer units) is soluble.[2,20] It is probably no coincidence, therefore,

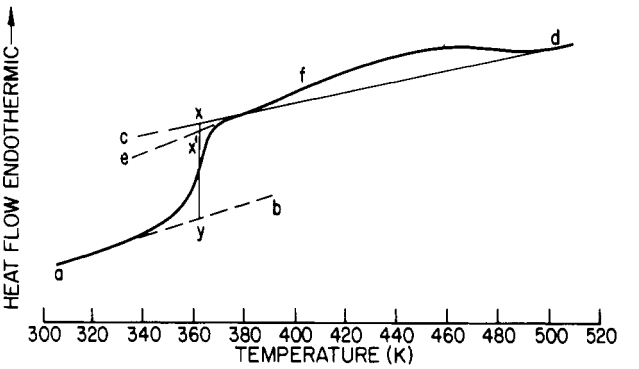

Figure 6. Measurement of heat capacity increment of PVC. Line ayb is heat capacity base line in glassy state. Line ex'f is base line in liquid state with melting included. Line cxd is base line in liquid state without melting included.

that long syndiotactic sequences have been essentially removed in this chlorine range (Figure 5). According to Fox and Schnecko,[15] for polymers whose distributions of diads obey Bernoullian trial statistics, the presence of only a small fraction of syndiotactic runs greater than a certain threshold length may be sufficient to insolubilize the greater portion of a polymer. Miller, who investigated the effect of sequence length and tacticity on crystallinity in polypropylene, concluded that for a random polymer his relationship reduced to eq 1 and that the quanity $f_{\geq N}$ was a measure of maximum crystallizability.[21]

We determined below using DSC data that our fused PVC contained 15% crystallinity. This corresponds essentially to the concentration (13%—see eq 4) of syndiotactic sequences in five or more monomer units. However, this is clearly not the maximum crystallizability of our PVC because the virgin powder gave 11.2 kJ/kg for a heat of melting. This corresponds to 21% crystallinity and indicates crystallization of syndiotactic sequences equal to and longer than four monomer units. Since Illers[22] has achieved heats of melting up to 20 kJ/kg for commerical PVC by annealing, it is evident that it is possible to involve even syndiotactic triads in crystallization.

Heat Capacity Change at T_g. In 1960 Wunderlich[23] reported the specific heat capacity increment (Δc_p) at T_g for a number of polymers. He observed the specific heat capacity increment times the average bead molecular weight ($\bar{M}$) equaled a constant, called the molar heat capacity (ΔC_p) per bead (eq 6). A bead was defined as the

$$\Delta C_p = \Delta c_p M = 11.3 \pm 2.1 \text{ kJ/(mol K)} \quad (6)$$

smallest molecular group whose movement may affect the state of the polymer. In the example of PVC, there are two beads per monomer unit, so $\bar{M} = 31.25$. The constant molar heat capacity rule has been updated and applied to other polymers.[24–26] The entire heat capacity increment was initially attributed to free volume expansion at T_g. Other workers have since proposed that conformational and vibrational effects also contribute to energy absorption at T_g.[27–31]

In the measurement of the heat capacity increment of PVC, a significant error can be introduced due to the very broad melting peak which extends down to the glass transition region (Figure 6). If the heat contribution from melting is not taken into account, the step change xy is underestimated by using instead height x'y. The difference XX' may amount to more than 10% depending on thermal history of the sample. This experimental difficulty may explain discrepancies among early measurements of Δc_p for PVC, which varied by as much as 100%.[33] More recent determinations give results of 0.29–0.33 J/(g K).[6,32,34]

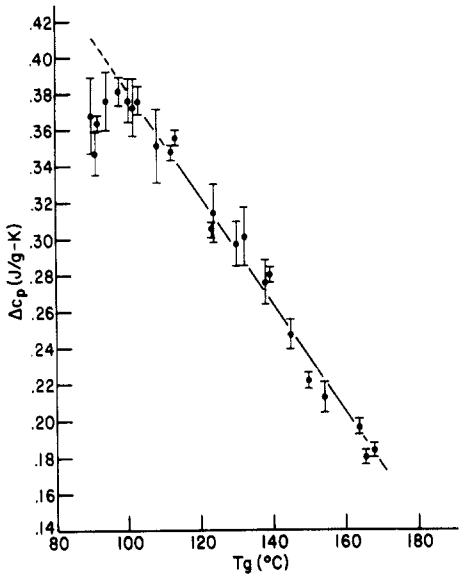

Figure 7. Specific heat capacity increment at T_g for solution-chlorinated PVC's.

In the case of PVC, and other partially crystalline polymers, the graphic procedure described above also suffers from another disadvantage. Specifically, even if the "amorphous" base line of the liquid state is drawn as line cd, the resultant value for Δc_p needs to be corrected further for the weight of the crystalline fraction, which does not contribute to the heat capacity change at T_g. As crystallinity increases, Δc_p decreases, and the relation is given by eq 7, where Δc_p° is the specific heat capacity increment for 100% amorphous polymer.[34]

$$X = 100[1 - (\Delta c_p/\Delta c_p^\circ)] \quad (7)$$

The Δc_p values for PVC and CPVC samples as measured in the second heat run are given in Table II and shown in Figure 7. The vertical bars represent standard deviations of from three to five measurements. Only the data for precipitated PVC samples are shown. The original, as-received powders had essentially the same value (Δc_p = 0.35 J/g K); see Table I). At first, the heat capacity increment rose to a maximum at about 59.5% chlorine (T_g about 100 °C) and then decreased linearly with T_g upon further chlorination. The initial rise in the heat capacity increment corresponds to the initial, rapid drop in crystallinity (Figure 1). This rise in Δc_p coincides, therefore, with the increase in mass of the amorphous-phase fraction.

The linear portion of the specific heat capacity vs. T_g relationship is fitted by eq 8, where T_g is in °C and the

$$\Delta c_p = 0.675 - (0.00294)(T_g)\ \text{J/(g °C)} \quad (8)$$

coefficient of determination (r^2) is 0.986. The increment for 100% amorphous PVC is estimated by substituting T_g = 91 °C for PVC in eq 8. The result is 0.408 J/(g K). Upon substituting this value and Δc_p = 0.355 J/(g K) (the average of three precipitated PVC samples) into eq 7, one obtains X = 13%. This value is used next to correct the observed T_g of PVC for its crystallinity. From the data of Ceccorulli et al.,[34] on the change in T_g with crystallinity, we determined an increase in T_g of 0.32 °C per percent crystallinity (X). Thus, the corrected T_g for 100% amorphous PVC is 87 °C, and from eq 8 the specific heat capacity increment is 0.419 J/(g K). This is about 33% higher than most reported values noted previously. The molar heat capacity per bead for PVC is $\Delta C_p = M\Delta c_p$ = (31.25)(0.419) = 13.1. Our value for PVC is slightly higher than the average value (11.3 ± 2.1 J/(mol K)) reported by Wunderlich, but still within experimental error of the latter.

Table V
PVC Specific Heat Capacity Increments (J/(g K)) at T_g

Δc_p^{fv}	Δc_c	Δc_{vbr}	Δc_p theory	Δc_p exptl
0.130	0.185[a]	0.122[a]	0.437[b]	0.419[d]
0.096	0.192	0.074	0.362[c]	0.419[d]

[a] Average of isotactic and syndiotactic configurations. [b] Roe and Tonelli.[30] [c] DiMarzio and Dowell.[29] [d] This work.

Table VI
Corrections to Heat Capacity Increments (J/(g K))

T_g, K	Δc_p[a]	$\Delta(\Delta c_c)$[b]	Δc_p(cor)	Δc_p(obsd)
373	0.396	0.009	0.387	0.380
393	0.362	0.026	0.336	0.323
413	0.334	0.041	0.293	0.265
433	0.309	0.054	0.255	0.205
443	0.298	0.061	0.236	0.176

[a] Calculated from $\Delta c_p = \Delta C_p/\bar{M}$. [b] Calculated from eq 11.

The percent crystallinity, as recalculated according to eq 7, using Δc_p° = 0.419 is 15%. This is higher than some typical values for PVC crystallinity, but in agreement with Guerrero et al.,[35] who examined the determination of PVC crystallinity by X-ray diffraction and concluded that reported values less than 10% for commercial PVC were too low. The heat of melting (ΔH_m°) for 100% crystalline PVC is calculated as 8.0/0.15 = 53.3 kJ/kg. This is comparable to some reported values,[36] but significantly less than the 78.6 kJ/kg value determined by Gouinlock[37] for a more highly crystalline PVC (X = 43%). For the latter, one would expect a higher ΔH_m° than our sample because of fewer defects.

Components of the Heat Capacity Change at T_g. As noted above, recent investigators[27-31] have suggested the heat capacity increment depends on contributions from conformational and vibrational effects as well as free volume changes. The total increment is given as

$$\Delta c_p = \Delta c_p^{fv} + \Delta c_c + \Delta c_{vbr} \quad (9)$$

where Δ_{cp}^{fv} is the free volume contribution, Δc_c is the conformational effect, and Δc_{vbr} is the vibrational effect.

Our experimental result for Δc_p° for amorphous PVC is compared in Table V with reported theoretical calculations and is in good agreement with the Roe–Tonelli calculation.[30] The agreement with the other theoretical result is within the 20% estimated error[29] of the latter. According to the Roe–Tonelli calculation, about 30% of the increment in PVC arises from free volume expansion, 42% from unfrozen conformational motions, and 28% from vibrational effects. The occurrence of conformational motions in PVC at T_g is supported by infrared data.[38]

According to eq 6, the specific heat capacity increment should decrease as the mass of a bead increases. The values for CPVC corrected for the mass effect are given in column 2 of Table VI. An additional correction is also made to take into account the effect of the higher T_g, namely, that a greater fraction of chains in the glassy state would occupy higher energy gauche states, thus contributing less to Δc_p.[28] The conformational heat capacity was given by eq 10, where f is the fraction of higher energy

$$\Delta c_c = Rf(1 - f)(\epsilon/kT)^2 \quad (10)$$

states, and ϵ is the energy difference between gauche and trans states. Since f and ϵ are unknown for CPVC's, we assume they are the same as for PVC. Actually, one might expect the energy difference in conformational states to

be greater for CPVC than PVC owing to additional steric and electrostatic effects of neighboring chlorine atoms. Using 0.185 J/(g K), the conformational heat capacity contribution for PVC determined by Roe and Tonelli,[30] and combining the two expressions for PVC and CPVC from eq 10, one obtains eq 11 as the difference, $\Delta(\Delta c_c)$, in

$$\Delta(\Delta c_c) = 0.185[1 - (T_g/T_g')^2] \quad (11)$$

conformational heat capacities between PVC and CPVC, where T_g is the glass transition temperature of PVC in kelvin and T_g' is the value for CPVC. The results are given in column 3 of Table VI. Column 4 contains the result corrected for both mass and temperature effects. It can be compared with interpolated results in column 5 taken from Figure 7.

Even after corrections for the mass and temperature effects, the experimentally determined heat capacity increments for CPVC lay significantly below the calculated values. We suggest the difference is a result of greater chain stiffness, and hence a lower than expected conformational heat capacity (Δc_c), when a hydrogen atom is replaced by a chlorine atom. We also conclude that the thermal behavior of CPVC at T_g cannot be treated simply as the sum effect of isolated CH_2, CHCl, and CCl_2 groups. A similar nonadditive effect on the molar heat capacity increment of brominated poly(2,6-dimethyl-1,4-phenylene oxides) was reported recently by Bopp et al.[39]

Other experimental evidence has been obtained to support the chain-stiffening argument for CPVC mentioned above. We previously measured the ^{13}C spin–lattice relaxation time (T_1) in solution for a 66% chlorine CPVC.[5] Carbon-13 T_1's are sensitive probes of high-frequency segmental motion at different sites on the polymer backbone or side chain.[40] For CPVC in solution under the conditions of the analysis,[5] a reduction in T_1 corresponds to a decrease in segmental mobility, i.e., a chain stiffening at that point. We found that the average T_1's of the central CH carbons of {010}, {110}, and {111}, respectively, decreased in the order 0.34, 0.27, and 0.25 s. Hence segmental mobility decreases with increasing chlorine substitution on CH_2 carbons. Also, methylene carbons next to adjacent CHCl sequences in CPVC have reduced T_1's relative to the methylene carbons in the unchlorinated PVC segments. The same is probably true when CCl_2 carbons are formed. However, we cannot confirm this directly for CCl_2 carbons since the T_1's of nonprotonated sites are difficult to interpret in terms of segmental motion. It is not unreasonable to expect the motional behavior in solution to be qualitatively similar to that in the melt.

We have also found the thermal properties of CPVC's do not conform to the Simha–Boyer relationship,[41] which states that the $(\Delta c_p)(T_g)$ = constant (about 115 J/g). From the data in Table II we calculated that this product decreased continuously from 140 to 80 J/g.

Molar Heat Capacities below and above T_g. The heat capacity of a polymer in the glass state arises solely from vibrational motions if the temperature is well below the T_g.[23] Wunderlich et al.[24,42] and others[26] have shown that constituent groups contribute additively to the molar heat capacity (C_p). For example, the heat capacity of PVC is made up of equimolar contributions of CH_2 and CHCl groups. On the other hand, CPVC would be characterized by fractional contributions from CH_2, CHCl, and CCl_2 groups. The molar heat capacities for PVC, and CPVC's (samples 3 and 18), are shown in Figure 8. Up to 340 K our results for PVC agree within 1% of those reported by Chang[43] using adiabatic calorimetry. The reproducibility of our values was 1–1.5% for PVC, 1.5–2.0% for LCPVC (sample 3), and 2–3% for CPVC (sample 18).

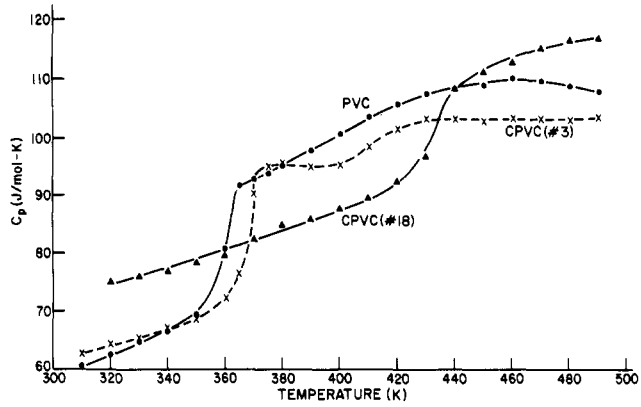

Figure 8. Molar heat capacities of PVC and CPVC's (samples 3 and 18).

Table VII
Heat Capacity Slope below and above T_g

resin	dC_p/dT, J/(mol K²) $<T_g$	dC_p/dT, J/(mol K²) $>T_g$
PVC	0.18 ± 0.03	0.261 ± 0.004
LCPVC[3]	0.17 ± 0.02	0.034 ± 0.028
CPVC[18]	0.166 ± 0.002	0.147 ± 0.005

According to Chang,[43] the slope (dC_p/dT) of the molar heat capacity for liquid PVC is about 0.355 J/(mol K²). This value is higher than that (0.16 J/(mol K²)) of glassy PVC, an observation noted for other crystalline polymers. This behavior has been attributed to the additional heat increment from crystallites melting just above T_g. The dC_p/dT results in this work are given in Table VII. The slope value (0.18 J/(mol K²)) below T_g determined for PVC agrees within experimental error with that reported by Chang. Our result above T_g is, however, significantly different probably because of a different thermal history.

The three chlorine-containing polymers in this study had the same slopes below T_g, but differed significantly above T_g. The behavior of the LCPVC is interesting in view of its other thermal properties. Its slope above T_g is less than that below T_g, which is typical of amorphous polymers.[26,29] This result is consistent with its low level of residual crystallinity (25% of that of PVC). It is evident that the residual crystallinity in sample 3 was not manifested as melting until about 400 K (Figure 8).

The dC_p/dT value for the CPVC above T_g falls between those of PVC and LCPVC. The fact that the heat capacity slope in the melt increased again as chlorine substitution went up may be a consequence of more structural order. This seems plausible in view of the evidence indicating increasing chain stiffness with greater chlorine substitution.

Registry No. PVC (homopolymer), 9002-86-2.

References and Notes

(1) Bier, G. *Kunststoffe* **1965**, *55*, 694.
(2) Trautvetter, W. *Kunstst-Plast (Solothurn, Switz.)* **1966**, *13*, 54.
(3) Keller, F.; Hosselbarth, B. *Faserforsch. Textiltech.* **1978**, *29*, 152 and references therein.
(4) Lukas, R.; Svelty, J.; Kolinsky, M. *J. Polym. Sci., Polym. Chem. Ed.* **1981**, *19*, 295 and references therein.
(5) Komoroski, R. A.; Parker, R. G.; Lehr, M. H. *Macromolecules* **1982**, *15*, 844.
(6) Wilski, H. *Kolloid Z. Z. Polym.* **1970**, *238*, 426.
(7) Bonnebat, C.; DeVries, A. J. *Polym. Eng. Sci.* **1978**, *18*, 824.
(8) Hosselbarth, B.; Keller, F.; Rehor, H.; Reicherdt, W. *Plaste Kautsch.* **1977**, *24*, 32.
(9) Hosselbarth, B.; Keller, F.; Tannert, F.; Reicherdt, W. *Acta Polym.* **1979**, *30*, 478.
(10) Komoroski, R. A.; Parker, R. G.; Shockcor, J. P. *Macromolecules*, preceding paper in this issue.
(11) Dorrestijn, A.; Lemstra, R. J. *Polym. Commun.* **1983**, *24*, 226.

(12) Carman, C. J. *Macromolecules* **1973**, *6*, 725.
(13) Pham, Q. T.; Millan, J. L.; Madruga, E. L. *Makromol. Chem.* **1974**, *175*, 945.
(14) Lemstra, P. J.; Keller, A.; Cudby, M. *J. Polym. Sci., Polym. Phys. Ed.* **1978**, *16*, 1507.
(15) Fox, T. G.; Schnecko, H. W. *Polymer* **1962**, *3*, 575.
(16) Manson, J. A.; Iobst, S. A.; Acosta, R. *J. Macromol. Sci., Phys.* **1974**, *B9*, 301.
(17) Guerrero, S. J.; Keller, A.; Soni, P. L.; Geil, P. H. *J. Macromol. Sci., Phys.* **1981**, *B20*, 161.
(18) Guerrero, S. J.; Keller, A. *J. Macromol. Sci., Phys.* **1981**, *B20*, 167.
(19) Small, P. A. *J. Appl. Chem.* **1953**, *3*, 71.
(20) Kaltwasser, H.; Klose, W. *Plaste Kautsch.* **1966**, *13*, 583.
(21) Miller, R. L. *J. Polym. Sci.* **1962**, *57*, 975.
(22) Illers, K. H. *J. Macromol. Sci., Phys.* **1977**, *B14*, 471.
(23) Wunderlich, B. *J. Phys. Chem.* **1960**, *64*, 1052.
(24) Wunderlich, B.; Jones, L. D. *J. Macromol. Sci., Phys.* **1969**, *B3*, 67.
(25) Brown, D. W.; Wall, L. A. *J. Polym. Sci., Part A-2* **1969**, *7*, 601.
(26) Wong, K. C.; Chen, F. C.; Choy, C. L. *Polymer* **1975**, *16*, 85.
(27) Goldstein, M. *J. Chem. Phys.* **1977**, *67*, 2246.
(28) O'Reilley, J. M. *J. Appl. Phys.* **1977**, *48*, 4043.
(29) DiMarzio, E. A.; Dowell, F. *J. Appl. Phys.* **1979**, *50*, 6061.
(30) Roe, R. J.; Tonelli, A. E. *Macromolecules* **1979**, *128*, 878.
(31) Tanaka, N. *Polymer* **1979**, *20*, 593.
(32) Illers, K. H. *Makromol. Chem.* **1969**, *127*, 1.
(33) Grewer, T.; Wilski, H. *Kolloid Z. Z. Polym.* **1970**, *238*, 426 and references therein.
(34) Ceccorulli, G.; Pizzoli, M.; Pezzin, G. *J. Macromol. Sci., Phys.* **1977**, *B14*, 499.
(35) Guerrero, S. J.; Meader, D.; Keller, A. *J. Macromol. Sci., Phys.* **1981**, *B20*, 185.
(36) "Polymer Handbook"; Brandrup, J., Imerugt, E. H., Eds.; Wiley: New York, 1975; Chapter V-7.
(37) Gouinlock, E. V. *J. Polym. Sci., Phys. Ed.* **1975**, *13*, 1533.
(38) Koenig, J. L.; Antoon, M. K. *J. Polym. Sci., Phys. Ed.* **1977**, *15*, 1379.
(39) Bopp, R. C.; Gaur, U.; Kambour, R. P.; Wunderlich, B. *J. Therm. Anal.* **1982**, *25*, 243.
(40) Komoroski, R. A.; Mandelkern, L. "Applications of Polymer Spectroscopy"; Brame, E. G., Jr., Ed.; Academic Press: New York, 1978; p 57.
(41) Boyer, R. F. *Macromol. Sci., Phys.* **1973**, *B7*, 487.
(42) Wunderlich, B.; Gaur, V. *Pure Appl. Chem.* **1980**, *52*, 445.
(43) Chang, S. S. *J. Res. Natl. Bur. Stand. (U.S.)* **1977**, *82*, 9.

Extension of Thermal Field-Flow Fractionation to Ultrahigh (20×10^6) Molecular Weight Polystyrenes

Yu S. Gao, Karin D. Caldwell, Marcus N. Myers, and J. Calvin Giddings*

Department of Chemistry, University of Utah, Salt Lake City, Utah 84112.
Received July 10, 1984

ABSTRACT: The theory and practice of thermal field-flow fractionation (thermal FFF) as a tool for characterizing the molecular weight distribution of polymers are reviewed and a number of advantages with respect to size exclusion chromatography (SEC or GPC) are summarized. Retention values are measured and tabulated for linear polystyrenes in THF in the molecular weight range 5.1×10^4 to 20.6×10^6. For calibration purposes, it is shown that a plot of the logarithm of the product of retention parameter λ and temperature drop ΔT vs. the logarithm of molecular weight is linear for this entire experimental range with a slope of −0.53. To demonstrate fractionation and the absence of shear degradation in the higher molecular weight range, a fraction was cut from the 20.6M peak, reinjected, and observed to elute as a narrow peak centered near the position of the cut. Calculations based on nonequilibrium theory show that column band broadening for a 20.6M peak eluted at $\Delta T = 8$ °C contributes only about 10% to the plate height, the remainder arising from the fractionation of the molecular weight distribution. Thus a molecular weight distribution curve was obtained. We found the latter to be characterized by $M_w/M_n \cong 1.52$. We conclude that thermal FFF is applicable to ultrahigh molecular weight polymers but that other FFF subtechniques, especially flow FFF and sedimentation FFF, may also work in this molecular weight range.

Introduction

Field-flow fractionation (FFF) is a family of high-resolution techniques that has proven applicable to the analytical fractionation of a very wide range of aqueous and nonaqueous systems of macromolecules, colloidal particles, and even larger particles.[1-5] FFF is a flow-elution method, like chromatography, but differential retention is achieved by the application of an external field or gradient perpendicular to the narrow, ribbon-like flow channel. The most common fields and gradients are provided by centrifugation or gravity (sedimentation FFF), a liquid cross-flow (flow FFF), electrical fields (electrical FFF), and temperature gradients (thermal FFF). Each of these subtechniques has its own unique characteristics and applicability.

Thermal FFF has proven to be the most useful subtechnique for lipophilic polymers; the polymer molecular weight distribution can be obtained from the fractionation pattern.[6-8] Currently, most polymer molecular weight determinations are performed by size exclusion chromatography (SEC or GPC).[9] In SEC, the elution range is narrowly limited to values between the interstitial volume of the column and the total liquid volume. This confined range limits the number of components which can be resolved by a given column.[10] By contrast, with FFF there is no inherent limit to the elution volume range, allowing an increased number of resolvable peaks. In addition, the field strength in FFF can be varied between runs or within a run (programming) to provide maximum adaptability to sample type, in contrast to the rather rigid range of applicability of any given SEC column. Furthermore, the fractionating power of FFF is several times that of SEC for a given number of theoretical plates.[10]

For ultrahigh molecular weight polymers, SEC is also hampered by the shear degradation of polymer chains in the high-shear flow of the packed bed.[11-13] Since velocity gradients in the open FFF channel are perhaps an order of magnitude less than those in high-performance SEC columns, and since extensional shear is virtually absent, shear problems should be greatly reduced in FFF.

In our previous work, the relationship between sample molecular weight and thermal FFF retention was explored for a variety of different polymers, e.g., linear poly-

0024-9297/85/2218-1272$01.50/0